Published in final edited form as:
Neuroimage. 2009 January 15; 44(2): 312–318. doi:10.1016/j.neuroimage.2008.09.02.

Metabolic imaging of rat brain during pharmacologically-induced tinnitus

A.K. Paul[a,b,*,†], **E. Lobarinas**[c,†], **R. Simmons**[c,d], **D. Wack**[a,c,e], **John C. Luisi**[a], **J. Spernyak**[f], **R Mazurchuk**[f], **H. Abdel-Nabi**[a], and **R. Salvi**[c]

a *Department of Nuclear Medicine, State University of New York, University at Buffalo, Buffalo, NY, USA*

b *Rochester General Hospital, Rochester, NY, USA*

c *Center for Hearing and Deafness, State University of New York, University at Buffalo, Buffalo, NY, USA*

d *Department of Neurology, State University of New York, University at Buffalo, Buffalo, NY, USA*

e *Buffalo Neuroimaging Analysis Center, State University of New York, University at Buffalo, Buffalo, NY, USA*

f *Preclinical Imaging Resource, Roswell Park Cancer Institute, Buffalo, NY, USA*

Abstract

Although much is known about the perceptual characteristics of tinnitus, its neural origins remain poorly understood. We investigated the pattern of neural activation in central auditory structures using positron emission tomography (PET) imaging in a rat model of salicylate-induced tinnitus. Awake rats were injected with the metabolic tracer, fluorine-18 fluorodeoxyglucose (FDG), once in a quiet state (baseline) and once during salicylate-induced tinnitus. Tinnitus was verified using a behavioral technique. Brain imaging was performed using a high-resolution microPET scanner. Rats underwent magnetic resonance imaging (MRI) and reconstructed MRI and microPET images were fused to identify brain structures. FDG activity in brain regions of interest were quantified and compared. MicroPET imaging showed that FDG activity in the frontal pole was stable between baseline and tinnitus conditions, suggesting it was metabolically inert during tinnitus. Inferior colliculi (p=0.03) and temporal cortices (p=0.003) showed significantly increased FDG activity during tinnitus relative to baseline; activity in the colliculi and temporal cortices increased by 17% ± 21% and 29% ± 20%, respectively. FDG activity in the thalami also increased during tinnitus, but the increase did not reach statistical significance (p=0.07). Our results show increased metabolic activity consistent with neuronal activation in inferior colliculi and auditory cortices of rats during salicylate-induced tinnitus. These results are the first to show that microPET imaging can be used to identify central auditory structures involved in tinnitus and suggest that microPET imaging might be used to evaluate the therapeutic potential of drugs to treat tinnitus.

*Corresponding author: Department of Nuclear Medicine, State University of New York, University at Buffalo,105 Parker Hall, 3435 Main St., Buffalo, NY, 14214, USA, Fax: +1 716 829 2980, E-mail: asit.paul@viahealth.org.
†These authors contributed equally to this work

Introduction

Subjective tinnitus, the perception of a phantom sound in the absence of an acoustic stimulus, affects approximately 3% of the population; however among those over the age of 65 the percentage rises to nearly 9% (Adams et al., 1999; Meikle, 1997). Tinnitus can be extremely disruptive and debilitating, leading many patients to seek medical attention. Tinnitus is generally associated with hearing loss resulting from aging or noise exposure (Nicolas-Puel et al., 2002). Since the phantom sound of tinnitus is generally perceived as originating in the ear with hearing loss, the neural generator responsible for tinnitus has traditionally been thought to reside in the inner ear. However, surgical removal of the auditory nerve connecting the inner ear to the auditory brain fails to abolish tinnitus in the majority of subjects (House and Brackmann, 1981). These results suggested that tinnitus might originate in the central auditory system. Support for a central generator of tinnitus has emerged from a number of brain imaging studies showing aberrant neural activity within the central auditory pathway of tinnitus patients (Cacace et al., 1994; Lockwood et al., 1998).

Identifying the underlying neural mechanisms that give rise to tinnitus in humans is difficult because of the lack of control over subject variables, etiology and difficulties measuring the neurochemical and biological factors associated with tinnitus. To circumvent these problems, researchers have developed animal models that can report on whether animals experience transient or permanent tinnitus following exposure to ototoxic drugs or high intensity noise (Guitton et al., 2003; Heffner and Harrington, 2002; Jastreboff et al., 1988; Lobarinas et al., 2004). One of the most reliable and well-studied inducers of tinnitus is sodium salicylate, the active ingredient in aspirin. High doses of salicylate induce tinnitus in humans and animals in a predictable, dose-dependent manner (Boettcher and Salvi, 1991; Jastreboff et al., 1988; Yang et al., 2007). Electrophysiological studies have identified salicylate-induced changes at several sites along the auditory pathway in anesthetized animals, but none have provided a global overview of the functional changes that occur along the auditory pathway in conscious animals that experience tinnitus.

Recent developments in high resolution, dedicated small animal positron emission tomography (PET) systems (microPET) make it possible to investigate neural activity throughout the brain in commonly used animal models (Kornblum et al., 2000; Mir et al., 2004). During neuronal activation, increased glucose consumption is required by the ATP-dependent Na+-K+ pumps to restore transmembrane ionic gradients following depolarization associated with action potentials and synaptic activity (Mata et al., 1980). Previous studies have shown that fluorine-18 fluoro-2-deoxyglucose (FDG), a glucose analogue, can be used to image neural activation in the brain (Kornblum et al., 2000; Mir et al., 2004). FDG is taken up by cells as a function of neuronal/metabolic activation and due to its irreversible phosphorylation remains trapped within these cells for hours. Moreover, anesthesia administered 40 min after FDG administration had no effect on the uptake of FDG into various brain regions when compared to results from conscious rats (Friston et al., 2007). Consequently, awake-animals can be injected with FDG during the presentation of an external or internal stimulus that activates the brain and anesthetized and imaged with microPET after a period of 40 minutes to obtain a ‘snap-shot’ of FDG distribution and reveal the pattern of brain activity during the awake and stimulated state.

The goal of the present study was to use microPET and FDG to assess the pattern of neural activity in major auditory processing areas in the brain before and during transient tinnitus induced by sodium salicylate. To accomplish this goal, we employed a behavioral paradigm and identified a dose of sodium salicylate that reliably induced tinnitus in rats. Afterwards, microPET and FDG were used to identify the level of metabolic activation in central auditory

structures when rats were sequestered in a sound-attenuating chamber (1) without tinnitus and (2) during salicylate-induced tinnitus.

Materials and methods

Subjects

All studies were approved and performed in accordance with the Institutional Animal Care and Use Committee at the University at Buffalo. Fifteen adult male Sprague Dawley rats (3–5 months, 300–500 g) were obtained from Charles River Laboratories (Wilmington, MA). Two groups (n=3 in each group) of rats were used to optimize the microPET image acquisition protocol (group 1) and verify the repeatability of the microPET data (group 2). A separate group of 9 rats (group 3) underwent microPET imaging to investigate the metabolic activation in the brain before (baseline) and following salicylate treatment (tinnitus). Because of scheduling constraints, only a subset of rats in this group underwent behavioral testing (n=6) and magnetic resonance imaging (MRI) (n=2).

Behavioral testing

A validated behavioral technique, known as schedule-induced polydipsia avoidance conditioning (SIP-AC), was used to determine the dose of salicylate that would reliably induce tinnitus in rats. Details of the methods can be found in our earlier publications (Lobarinas et al., 2004; Lobarinas et al., 2006). Briefly, rats were food deprived to 90% normal body weight but had free access to water in their home cage. During experimental sessions rats were first trained to lick for water at high rate even though they were not thirsty (polydipsia) by delivering a food-pellet automatically every 60 s. Afterward, this licking behavior was put under stimulus control using avoidance conditioning. Rats were only allowed to lick for water during 30 s intervals of no sound (quiet) that were randomly interspersed among 30 s intervals of sound (4, 8, 12, 16, or 20 kHz narrow band noise, 100 Hz bandwidth, or 16 kHz pure tone, 40–60 dB SPL). Licks that occurred during sound intervals resulted in the delivery of brief intermittent foot shock. After two to three weeks of training, rats correctly discriminated quiet intervals (>90% correct responses) from sound interval (<10% incorrect responses). In daily 2-h test sessions, licks in quiet averaged 2000–4000 licks while licks in sound remained low, typically less than 100 licks. Rats were then treated for two consecutive days with intraperitoneal (i.p.) injections of saline or 50, 100, 150, 250 or 350 mg/kg of sodium salicylate (Sigma-Aldrich Corp, St. Louis, MO). Behavioral testing commenced 1 h post-injection. Dosing was administered in a pseudorandom order with a one week washout period. No abnormalities in weight, pellet consumption or behavior were observed during testing.

MicroPET image acquisition

A high resolution, animal PET scanner (Focus 120® microPET, Siemens Preclinical Solution, Knoxville, TN) was used to image the rat brain. The scanner, with 96 lutetium oxyortho-silicate detectors, has a spatial resolution of 1.3 mm at the center of the field of view (FOV), a volumetric resolution of 2.5 μL and an axial FOV of 7.6 cm. Details of the performance characteristics of the scanner have been described previously (Tai et al., 2005). For each imaging session, awake rats were injected with 74 MBq of FDG i.p. into the right lower quadrant of the abdomen. Each rat was initially anesthetized with 5% isofluorane (Minrad Inc, Bethlehem, PA) in an induction chamber. Afterwards, the rat was placed in the scanner bed in the prone position with the long axis of the rat's head parallel to the long-axis of the scanner and within the FOV of the scanner. During image acquisitions, rats were anesthetized with 1–2% isofluorane gas delivered through a custom face mask. For Group 1, dynamic image acquisition, in which a set of serial PET images were collected to assess influx of the tracer over time was started immediately after the injection of FDG and lasted 90 min (9 frames, 10 min each). For Group 2, static image acquisition, in which tracer had reached a steady state

level in the brain, was started 45 min following FDG administration and images were acquired for 45 min. To demonstrate the repeatability of the data, images were acquired identically in this group 48 h later. For Group 3, rats were imaged on two separate days to obtain baseline and tinnitus scans. On day 1, static baseline images of rats were acquired 45 min after the injection of FDG. On day 3, rats were first injected i.p. with 250 mg/kg of sodium salicylate followed 1 h later by administration of FDG. Forty-five min later, static tinnitus images were acquired for 45 min. Rats in Groups 2 and 3 were kept in a sound-attenuating cubicle during the interval between the administration of FDG and image acquisition.

MRI acquisition

Once the microPET imaging experiments were completed and radioactivity was decayed, 2 rats in group 3 underwent MRI on a separate day. MRI was carried out on a 4.7 Tesla MR scanner using a 72 mm quadrature transceiver coil (Bruker Biospin, Billerica, MA). Anesthesia was induced in the rats with 4% isofluorane and maintained with 1–2% isofluorane during imaging. The respiratory rate and body temperature of rats were monitored with an MR-compatible monitoring & gating system (Model 1025, SA Instruments, Inc., Stony Brook, NY). Animal temperature was maintained at 37° C during the scan by blowing heated air onto the animals. Following acquisition of scout images to determine location and orientation of brain within the scanner, a T2-weighted, three-dimensional fast spin echo scan was acquired in the coronal orientation. Scanning parameters of the high-resolution, T2-weighted scan were as follows: effective echo time, 85 ms; repetition time, 3 s; field of view, 40 × 40 × 40 mm; matrix size, 128 × 128 × 96 and echo train length, 16, 2 averages). Raw data was zero-filled to a 160^3 matrix, and transformed to image data via Fourier Transform to achieve an isotropic digital resolution of 250 microns.

Image analysis and quantification

MicroPET images were reconstructed with the standard filtered back-projection method. Reconstructed images were displayed in transverse, coronal and sagittal planes. A total of 128 sequential tomographic slices were displayed over the imaging object of interest with each slice measuring 0.087 mm in thickness. The scans from the rats which had both PET and MRI (T1 and T2 weighted) were anatomically fused using the normalized mutual information routine taken from SPM5 (Collignon et al., 1995; Friston et al., 2007; Wells et al., 1996). Quantification of FDG activity was performed using the scanner's built-in ASIPRO ® software executed on the IDL Virtual Machine 6.0 platform. The first step in the analysis was quantification calibration that allowed conversion of image count density to an activity concentration. Calibration was performed by scanning a uniform cylindrical phantom with a known activity concentration, A (Bq/mL). From the reconstructed images, the average count density within a region of interest (ROI) in the central portion of the image, C (counts/voxel/s), was determined. Because the activity concentration in the phantom is known, the calibration factor (CF) between image counts and activity concentration was then: CF= A (Bq/mL × branching fraction/C (counts/voxel/s). For FDG the branching fraction is 0.977, which is the fraction of decays that occur via positron emission. Counts were obtained from each anatomical structure by drawing an ROI around the structure. The activity concentration in each ROI was obtained by applying the CF to the count in the ROI and was expressed as a fraction of the injected dose per unit volume of tissue (%ID/mL) as described previously (Yang et al., 2003). In addition, a count ratio (CR) was calculated by dividing the FDG count in a given structure divided by that in the frontal pole. The use of CR eliminated potential confounding factors such as dose-effect and calibration-effect that might be propagated through the data. Counts from three clearly identifiable structures in the central auditory pathway, temporal cortex (TCx), thalamus (TL) and inferior colliculus (IC), were computed. Average of counts obtained from ROI in the right and left TCx were combined into a single value. Counts from the TL and IC were determined using a single ROI that included both left and right sides.

Statistical Analysis

Data are expressed as mean values ± 1 SD. Comparisons between the paired data within a group were made using Student's paired t test. Correlations were tested using linear regression analysis. Data from the SIPAC behavioral measures were evaluated using a two-way repeated measures Analysis of Variance to determine the differences in lick counts following administration of salicylate and at baseline (Student-Newman-Keuls post-hoc analysis). A p value <0.05 was considered significant for all comparisons.

Results

Salicylate-Induced tinnitus

The mean data for baseline, saline and five salicylate conditions are shown in Fig. 1. During baseline testing, rats made ~3800 licks-in-quiet (>90% correct) and few licks-in-sound (<10%, 40 dB SPL). Afterwards, rats were injected with saline. During the saline-control condition, licks-in-quiet remained high, ~3700, and licks-in-sound remained low indicating that the injections had no adverse effects on performance. During the salicylate treatments, licks-in-sound remained low for all five salicylate doses ($p>0.05$). These results indicate that the rats could hear the real sound. With the 50 mg/kg dose of salicylate, licks-in-quiet remained high and similar to baseline, indicating an absence of tinnitus. Licks-in-quiet were slightly reduced by the 100 mg/kg salicylate dose. However, licks-in-quiet were significantly reduced relative to baseline during the 150, 250 and 350 mg/kg doses of salicylate ($p<0.05$). These results indicate that salicylate doses of 150 mg/kg or higher induce the phantom sounds of tinnitus. Based on these results, the 250 mg/kg dose of salicylate was used to induce tinnitus prior to FDG imaging.

Protocol Optimization (Group 1)

The dynamic microPET study showed that FDG began accumulating in the brain immediately after the injection, reached a peak between 30–45 min post-injection and remained at a plateau for the next 45 min (Fig. 2). All three rats imaged dynamically for 90 min showed a similar pattern. Thus, image acquisition beginning at 45 min after FDG injection and lasting for 45 min thereafter reflected peak FDG activity in the brain. Moreover, the dose of 74 MBq of FDG provided excellent images of the rat brain using this protocol.

Repeatability (Group 2)

The CR for TCx, TL and IC obtained from two sets of images acquired 48 h apart showed excellent agreement. The mean CR of the two image sets were not significantly different (1.02 ± 0.12 vs. 1.00 ± 0.14; p=0.78). Fig. 3A shows the individual CRs of the TCx, TL and IC obtained from the first image set plotted against the corresponding CRs from the second image set. Analysis of the results showed a strong linear and statistically significant correlation between the two sets of data (Pearson correlation coefficient, r = 0.81, p<0.01) (Fig. 3A). The Bland-Altman plot showing the differences versus averages of the two measurements did not reveal any trend of under or overestimation between measurements and the ranges of differences were within the 99% confidence interval (Fig. 3B). These data indicate that FDG measurements obtained from the same animal several days apart are highly reproducible and provide a basis for comparing FDG activity obtained during baseline versus tinnitus conditions.

Salicylate-Induced Tinnitus (Group 3)

Figure 4 shows representative MRI, fused MRI-PET and PET images of a study rat showing central auditory structures: TCx, TL and IC. Two representative microPET image sets of a rat brain during baseline and then during tinnitus induced by 250 mg/kg of sodium salicylate are shown in Fig. 5. Images were displayed in the same color scale. Visual comparison of the lower

and upper panel shows evidence of increased FDG uptake during salicylate-induced tinnitus in TCx, TL and IC and several other regions of the brain. Quantitatively, FDG activity in the frontal pole, expressed as %ID/mL, was minimal and did not change between baseline and tinnitus conditions (0.22 ± 0.09 vs. 0.20 ± 0.09; p=0.16) suggesting that this region was metabolically unaffected across conditions (Fig. 6A). Therefore FDG counts in the TCx, TL and IC were normalized to counts in the frontal pole to compute the CR. The CR values were used to determine the changes in FDG activity in central auditory structures during tinnitus relative to the baseline. The results are summarized in Table 1. Tinnitus-induced changes in FDG CR from the baseline for each of the 9 rats are shown in Fig. 6B. Most of the rats showed increase FDG activity in TCx, IC and TL. The mean FDG CR of TCx and IC were significantly higher during tinnitus than baseline; TL also showed higher FDG CR during tinnitus, but the differences did not reach statistical significance. The %ID/mL of FDG in these structures showed trends similar to the CR data (results not shown).

Discussion

Our SIP-AC behavioral data (Fig. 1) indicated that salicylate doses between 150 and 350 mg/kg significantly suppressed licks-in-quiet, behavior consistent with the perception of a phantom sound during quiet intervals. In contrast, saline and low-doses of salicylate (≤ 100 mg/kg) failed to produce tinnitus-like behavior. These results are consistent with our earlier behavioral data as well as with findings of others (Bauer et al., 1999;Guitton et al., 2003;Jastreboff et al., 1988;Lobarinas et al., 2004;Lobarinas et al., 2006;Ruttiger et al., 2003). We also demonstrated that FDG activity reached a peak at about 45 min after FDG administration and remained at a plateau for about 45 min. Thus, our imaging was acquired during the constant peak activity. Our repeatability study showed excellent agreement between the quantitative parameters obtained from two sets of images obtained from the same rats 48 h apart. This allowed us to compare the data at baseline and during tinnitus. The 250 mg/kg dose of salicylate used in our imaging studies was above the level needed to induce tinnitus-like behavior and did not produce any side effects. The 250 mg/kg dose of salicylate did not alter FDG activity in the frontal pole. Therefore the frontal pole was used to normalize the results from the structures in the auditory pathway. Treatment with 250 mg/kg salicylate significantly increased FDG activity, a measure of metabolic/neuronal activation, in the IC as well as in the TCx representing the auditory cortex (ACx). The FDG activity also increased in the TL after salicylate treatment; however, the increase fell slightly below the level of statistical significance. These results suggest the involvement of IC, possibly the TL, and the ACx in tinnitus activity and the pattern supports the hypothesis that abnormal neuronal activity is relayed through the sub-cortical auditory pathway and processed in the cortex. However, an alternative explanation for these findings is that activity changes in the ACx modulate neural activity involved with tinnitus in subcortical sites (Suga and Ma, 2003).

The activation of ACx in tinnitus perception, as has been shown in our study, is consistent with most published studies. Human PET imaging studies have linked the perception of noise or age-induced tinnitus to increased or asymmetric metabolic activity in a variety of different regions of the central nervous system including the left or right ACx, areas surrounding the ACx, the medial geniculate body adjacent to the TL, temporal-parietal auditory association areas, and limbic regions (Arnold et al., 1996; Giraud et al., 1999; Langguth et al., 2006; Lockwood et al., 1998; Lockwood et al., 2001; Reyes et al., 2002; Wang et al., 2001). Functional MRI studies with humans have also linked tinnitus to aberrant neural activity in the IC, medial geniculate body and ACx (Cacace et al., 1999; Lanting et al., 2008; Melcher et al., 2000; Smits et al., 2007). Magnetoencephalography studies have showed enhanced neural activity and altered tonotopic organization in ACx (Diesch et al., 2004; Wienbruch et al., 2006). In one study, transcranial magnetic stimulation (TMS) was used to reduce the observed hyperactivity in the auditory cortex. The amount of hypermetabolic activity in ACx before

treatment correlated significantly with the reduction in tinnitus severity after TMS treatment. (Langguth et al., 2006). The diverse activation sites seen in human imaging studies of tinnitus are likely to reflect uncontrolled subject variables or diverse etiology (age, noise exposure, tumor, ototoxic drug etc). In contrast, the mode of tinnitus induction and subject variables can be carefully controlled in animal studies of tinnitus, particularly when measurements are obtained from the same subject before and after tinnitus induction as was done here. Increases in spontaneous activity and neural synchrony have also been seen in neurons in secondary ACx of anesthetized cats treated with salicylate (Eggermont and Kenmochi, 1998). In a study evaluating both behavioral and physiological measures obtained from ACx of unanesthetized rats, salicylate induced tinnitus was correlated with enhanced amplitudes in ACx local field potentials and a decrease in spontaneous activity (Yang et al., 2007). Both the sound frequency at which enhancement occurred and the time course of the enhancement mirrored the changes observed behaviorally, suggesting that the increase ACx activity may be an indicator of tinnitus.

Only a few studies are available that examined the subcortical activation pattern in vivo during tinnitus. In one study, consistent with our results, high doses of salicylate significantly increase glucose and lactate levels in both the IC and ACx in rats (Liu et al., 2003). In another study, changes in metabolic activity in ACx and subcortical structures have been evaluated in gerbils using [carbon-14]2-deoxyglucose (2-DG) autoradiograpgy after a 4-day treatment with salicylate (200–350 mg/kg) (Wallhausser-Franke et al., 1996). Gerbils received 2-DG 2 h after the last dose of salicylate and were sacrificed 90 min later for autoradiography. Glucose uptake was increased in ACx but decreased in IC and other subcortical structures including cochlear nucleus and lateral lemniscus in salicylate-treated gerbils compared to that seen in saline-treated animals. Based on that data, the authors suggested that salicylate-induced tinnitus activated ACx without activation of the IC. This is in sharp contrast with our study where we observe an increased FDG uptake in ACx as well as in subcortical structures including IC and TL. A direct comparison of our study to the gerbil study is difficult because of a number of differences in study techniques that include species (rat vs. gerbil), dosing of salicylate (single vs. multiple) and method of assessment (microPET vs. autoradiography). In addition, microPET imaging allowed us to compare metabolic activity in the same rats before and after salicylate administration. Interestingly, a subsequent study from the same group demonstrated salicylate evoked c-fos expression indicative of neural excitation in the IC (Wallhausser-Franke, 1997). Our results of increased IC activation are also consistent with the results of other studies that have demonstrated increased spontaneous activity in the IC following treatment with high doses of sodium salicylate (Chen and Jastreboff, 1995; Jastreboff and Sasaki, 1986). Spontaneous rates of neurons in the external nucleus of the IC increased and many neurons had bursting discharge patterns. These changes were mainly seen in neurons tuned to 10–16 kHz, frequencies close to the pitch of tinnitus measured behaviorally. Others have reported that intravenous salicylate increased spontaneous rates in the IC in proportion to its serum concentrations (Manabe et al., 1997). Collectively, these results suggest that high doses of salicylate increase spontaneous activity in the IC and that this activity may be relayed to the ACx where it gives rise to the perception of tinnitus.

In conclusion, our results indicate that a high dose of salicylate that reliably induces behavioral evidence of tinnitus in rats is associated with a significant increase in metabolic activity in the ACx, IC and to a lesser extent the TL. These results also suggest that metabolic activity assessed through microPET might be used as a surrogate marker of neuronal activation linked to tinnitus. It is not known if the neurophysiological changes associated with salicylate induced tinnitus are the same as those associated with noise-induced tinnitus. Thus it would be important to determine if noise-induced tinnitus produced changes in FDG activity similar to those seen with salicylate. Future studies with microPET imaging might be used to evaluate the therapeutic benefits and sites of action of drugs to treat tinnitus. Finally, animal models have so far only

been used to document the perceptual auditory aspect of tinnitus, not its emotional impact. Future animal studies aimed at assessing the emotional aspects of tinnitus might prove informative since human imaging studies of tinnitus patients have found coactivation of nonauditory as well as auditory brain areas (Andersson et al., 2000; Lockwood et al., 1998; Mirz et al., 2000).

Acknowledgements

This research was supported in part by research grants awarded by the National Institute of Deafness and Other Communication Disorders (1R01 DC009091). Additional support was available from the American Tinnitus Association.

References

Adams PF, Hendershot GE, Marano MA. Current estimates from the National Health Interview Survey, 1996. Vital Health Stat 1999;10:1–203.

Andersson G, Lyttkens L, Hirvela C, Furmark T, Tillfors M, Fredrikson M. Regional cerebral blood flow during tinnitus: a PET case study with lidocaine and auditory stimulation. Acta Otolaryngol 2000;120:967–972. [PubMed: 11200593]

Arnold W, Bartenstein P, Oestreicher E, Romer W, Schwaiger M. Focal metabolic activation in the predominant left auditory cortex in patients suffering from tinnitus: a PET study with [18F] deoxyglucose. ORL J Otorhinolaryngol Relat Spec 1996;58:195–199. [PubMed: 8883104]

Bauer CA, Brozoski TJ, Rojas R, Boley J, Wyder M. Behavioral model of chronic tinnitus in rats. Otolaryngol Head Neck Surg 1999;121:457–462. [PubMed: 10504604]

Boettcher FA, Salvi RJ. Salicylate ototoxicity: review and synthesis. Am J Otolaryngol 1991;12:33–47. [PubMed: 2029065]

Cacace AT, Cousins JP, Parnes SM, Semenoff D, Holmes T, McFarland DJ, Davenport C, Stegbauer K, Lovely TJ. Cutaneous-evoked tinnitus. i Phenomenology, psychophysics and functional imaging. Audiol Neurootol 1999;4:247–257. [PubMed: 10436317]

Cacace AT, Lovely TJ, Winter DF, Parnes SM, McFarland DJ. Auditory perceptual and visual-spatial characteristics of gaze-evoked tinnitus. Audiology 1994;33:291–303. [PubMed: 7818383]

Chen GD, Jastreboff PJ. Salicylate-induced abnormal activity in the inferior colliculus of rats. Hear Res 1995;82:158–178. [PubMed: 7775282]

Collignon A, Maes F, Delaere D, Vandermeulen D, Suetens P, Marchal G. Automated multi-modality image registration based on information theory. Information Processing in Medical Imaging 1995;14:263.

Diesch E, Struve M, Rupp A, Ritter S, Hulse M, Flor H. Enhancement of steady-state auditory evoked magnetic fields in tinnitus. Eur J Neurosci 2004;19:1093–1104. [PubMed: 15009157]

Eggermont JJ, Kenmochi M. Salicylate and quinine selectively increase spontaneous firing rates in secondary auditory cortex. Hear Res 1998;117:149–160. [PubMed: 9557985]

Friston K, Ashburner J, Kiebel S, Nichols T, Penny W. Statistical parametric mapping: the analysis of functional brain images. 2007

Giraud AL, Chery-Croze S, Fischer G, Fischer C, Vighetto A, Gregoire MC, Lavenne F, Collet L. A selective imaging of tinnitus. Neuroreport 1999;10:1–5. [PubMed: 10094123]

Guitton MJ, Caston J, Ruel J, Johnson RM, Pujol R, Puel JL. Salicylate induces tinnitus through activation of cochlear NMDA receptors. J Neurosci 2003;23:3944–3952. [PubMed: 12736364]

Heffner HE, Harrington IA. Tinnitus in hamsters following exposure to intense sound. Hear Res 2002;170:83–95. [PubMed: 12208543]

House JW, Brackmann DE. Tinnitus: surgical treatment. Ciba Foundation Symposium 1981;85:204–216. [PubMed: 6915835]

Jastreboff PJ, Brennan JF, Coleman JK, Sasaki CT. Phantom auditory sensation in rats: an animal model for tinnitus. Behav Neurosci 1988;102:811–822. [PubMed: 3214530]

Jastreboff PJ, Sasaki CT. Salicylate-induced changes in spontaneous activity of single units in the inferior colliculus of the guinea pig. J Acoust Soc Am 1986;80:1384–1391. [PubMed: 3782617]

Kornblum HI, Araujo DM, Annala AJ, Tatsukawa KJ, Phelps ME, Cherry SR. In vivo imaging of neuronal activation and plasticity in the rat brain by high resolution positron emission tomography (microPET). Nat Biotechnol 2000;18:655–660. [PubMed: 10835605]

Langguth B, Eichhammer P, Kreutzer A, Maenner P, Marienhagen J, Kleinjung T, Sand P, Hajak G. The impact of auditory cortex activity on characterizing and treating patients with chronic tinnitus - first results from a PET study. Acta Otolaryngol Suppl 2006:84–88. [PubMed: 17114149]

Lanting CP, De Kleine E, Bartels H, Van Dijk P. Functional imaging of unilateral tinnitus using fMRI. Acta Otolaryngol 2008;128:415–421. [PubMed: 18368576]

Liu J, Li X, Wang L, Dong Y, Han H, Liu G. Effects of salicylate on serotoninergic activities in rat inferior colliculus and auditory cortex. Hear Res 2003;175:45–53. [PubMed: 12527124]

Lobarinas E, Sun W, Cushing R, Salvi R. A novel behavioral paradigm for assessing tinnitus using schedule-induced polydipsia avoidance conditioning (SIP-AC). Hear Res 2004;190:109–114. [PubMed: 15051133]

Lobarinas E, Yang G, Sun W, Ding D, Mirza N, Dalby-Brown W, Hilczmayer E, Fitzgerald S, Zhang L, Salvi R. Salicylate- and quinine-induced tinnitus and effects of memantine. Acta Otolaryngol Suppl 2006:13–19. [PubMed: 17114137]

Lockwood AH, Salvi RJ, Coad ML, Towsley ML, Wack DS, Murphy BW. The functional neuroanatomy of tinnitus: evidence for limbic system links and neural plasticity. Neurol 1998;50:114–120.

Lockwood AH, Wack DS, Burkard RF, Coad ML, Reyes SA, Arnold SA, Salvi RJ. The functional anatomy of gaze-evoked tinnitus and sustained lateral gaze. Neurol 2001;56:472–480.

Manabe Y, Yoshida S, Saito H, Oka H. Effects of lidocaine on salicylate-induced discharge of neurons in the inferior colliculus of the guinea pig. Hear Res 1997;103:192–198. [PubMed: 9007584]

Mata M, Fink DJ, Gainer H, Smith CB, Davidsen L, Savaki H, Schwartz WJ, Sokoloff L. Activity-dependent energy metabolism in rat posterior pituitary primarily reflects sodium pump activity. J Neurochem 1980;34:213–215. [PubMed: 7452237]

Meikle MB. Electronic access to tinnitus data: the Oregon Tinnitus Data Archive. Otolaryngol Head Neck Surg 1997;117:698–700. [PubMed: 9419101]

Melcher JR, Sigalovsky IS, Guinan JJ Jr, Levine RA. Lateralized tinnitus studied with functional magnetic resonance imaging: abnormal inferior colliculus activation. J Neurophysiol 2000;83:1058–1072. [PubMed: 10669517]

Mir HM, Tatsukawa KJ, Carmichael ST, Chesselet MF, Kornblum HI. Metabolic correlates of lesion-specific plasticity: an in vivo imaging study. Brain Res 2004;1002:28–34. [PubMed: 14988030]

Mirz F, Gjedde A, Sodkilde-Jrgensen H, Pedersen CB. Functional brain imaging of tinnitus-like perception induced by aversive auditory stimuli. Neuroreport 2000;11:633–637. [PubMed: 10718327]

Nicolas-Puel C, Faulconbridge RL, Guitton M, Puel JL, Mondain M, Uziel A. Characteristics of tinnitus and etiology of associated hearing loss: a study of 123 patients. Int Tinnitus J 2002;8:37–44. [PubMed: 14763234]

Reyes SA, Salvi RJ, Burkard RF, Coad ML, Wack DS, Galantowicz PJ, Lockwood AH. Brain imaging of the effects of lidocaine on tinnitus. Hear Res 2002;171:43–50. [PubMed: 12204348]

Ruttiger L, Ciuffani J, Zenner HP, Knipper M. A behavioral paradigm to judge acute sodium salicylate-induced sound experience in rats: a new approach for an animal model on tinnitus. Hear Res 2003;180:39–50. [PubMed: 12782351]

Smits M, Kovacs S, de Ridder D, Peeters RR, van Hecke P, Sunaert S. Lateralization of functional magnetic resonance imaging (fMRI) activation in the auditory pathway of patients with lateralized tinnitus. Neuroradiology 2007;49:669–679. [PubMed: 17404721]

Suga N, Ma X. Multiparametric corticofugal modulation and plasticity in the auditory system. Nat Rev Neurosci 2003;4:783–794. [PubMed: 14523378]

Tai YC, Ruangma A, Rowland D, Siegel S, Newport DF, Chow PL, Laforest R. Performance evaluation of the microPET focus: a third-generation microPET scanner dedicated to animal imaging. J Nucl Med 2005;46:455–463. [PubMed: 15750159]

Wallhausser-Franke E. Salicylate evokes c-fos expression in the brain stem: implications for tinnitus. Neuroreport 1997;8:725–728. [PubMed: 9106755]

Wallhausser-Franke E, Braun S, Langner G. Salicylate alters 2-DG uptake in the auditory system: a model for tinnitus? Neuroreport 1996;7:1585–1588. [PubMed: 8904760]

Wang H, Tian J, Yin D, Jiang S, Yang W, Han D, Yao S, Shao M. Regional glucose metabolic increases in left auditory cortex in tinnitus patients: a preliminary study with positron emission tomography. Chin Med J (Engl) 2001;114:848–851. [PubMed: 11780365]

Wells WM, Viola P, Atsumi H, Nakajima S, Kikinis R. Multi-modal volume registration by maximization of mutual information. Medical Image Analysis 1996;1:35–51. [PubMed: 9873920]

Wienbruch C, Paul I, Weisz N, Elbert T, Roberts LE. Frequency organization of the 40-Hz auditory steady-state response in normal hearing and in tinnitus. Neuroimage 2006;33:180–194. [PubMed: 16901722]

Yang G, Lobarinas E, Zhang L, Turner J, Stolzberg D, Salvi R, Sun W. Salicylate induced tinnitus: Behavioral measures and neural activity in auditory cortex of awake rats. Hear Res 2007;226:244–253. [PubMed: 16904853]

Yang H, Berger F, Tran C, Gambhir SS, Sawyers CL. MicroPET imaging of prostate cancer in LNCAP-SR39TK-GFP mouse xenografts. Prostate 2003;55:39–47. [PubMed: 12640659]

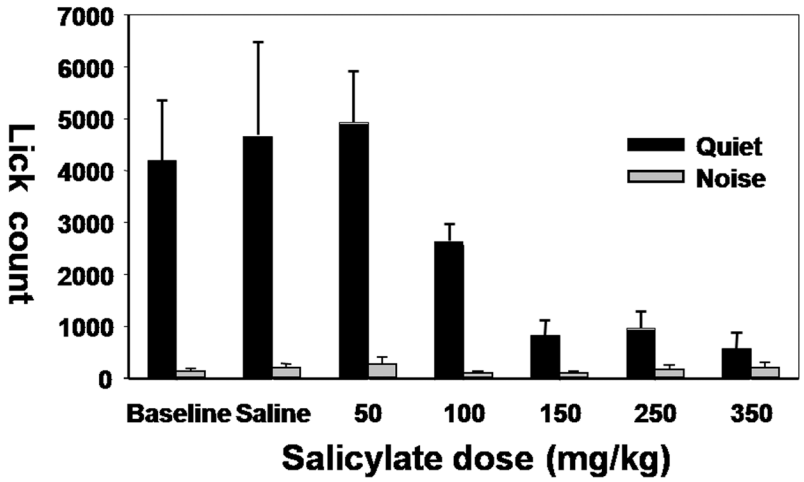

Fig. 1.

Lick counts by rats during quiet intervals (black) and noise intervals (gray) over a 2 h test period. Data are shown for baseline, saline and five doses of sodium salicylate ranging from 50 to 350 mg/kg. Compared to baseline, licks-in-quiet are significantly lower ($p<0.05$) with salicylate doses 150 mg/kg indicating presence of tinnitus. Licks-in-noise remained low and did not differ significantly from baseline ($p>0.05$) at all salicylate doses.

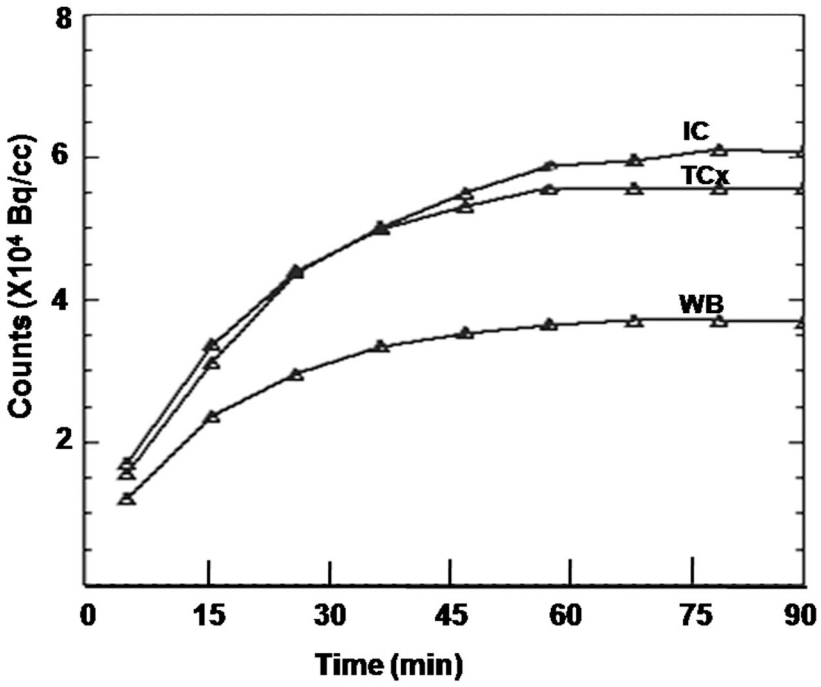

Fig. 2.

FDG counts over time in the inferior colliculi (IC) and temporal cortices (TCx) as well as in the whole brain (WB) obtained from a 90 min dynamic microPET scan of a rat immediately after the intraperitoneal injection FDG.

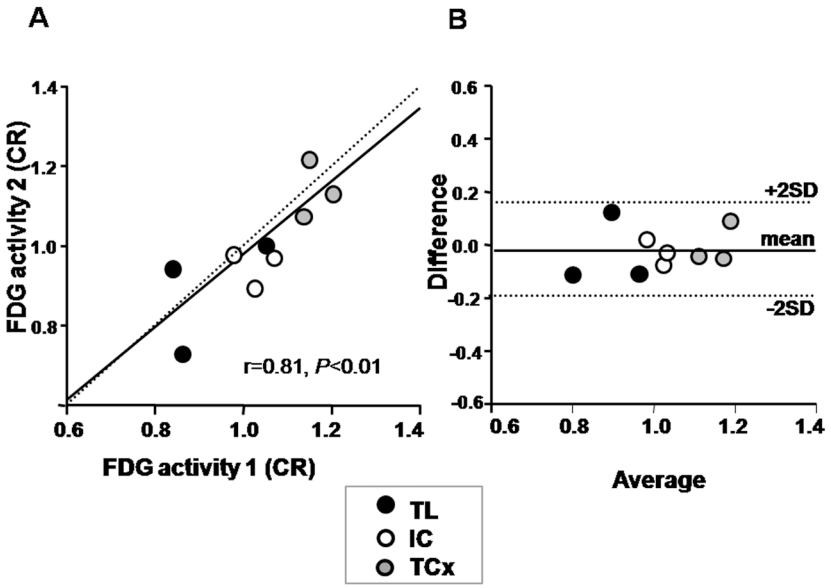

Fig. 3.

Scatter plot (A) and Bland Altman plot (B) showing excellent correlation and agreement between two sets of data acquired under identical conditions separated by 48 h. FDG activity is expressed as a count ratio (CR) between each region of interest and the frontal pole. CRs of temporal cortices (TCx), thalami (TL) and inferior colliculi (IC) in rats (Group 2) are shown as black, grey and white circles respectively. SD, standard deviation.

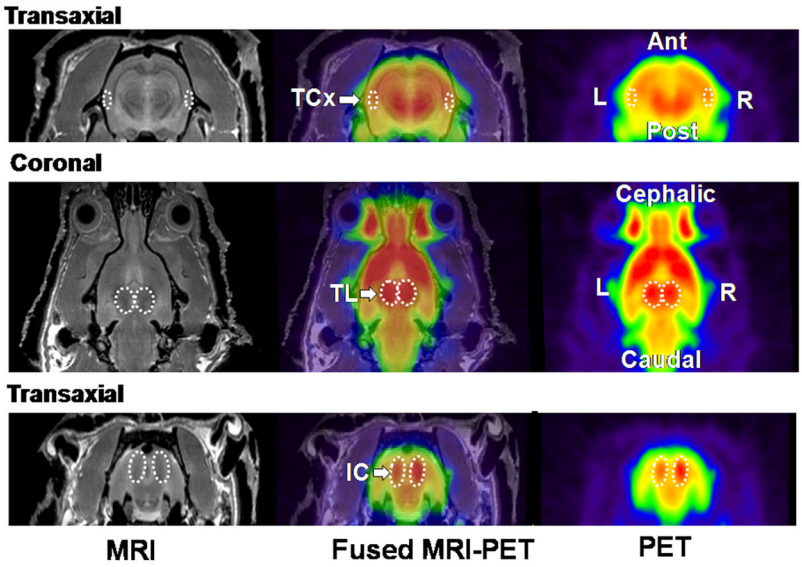

Fig. 4.

Corresponding transaxial and coronal images obtained from MRI (left column), fused MRI/microPET (middle column) and microPET (right column) of a rat. Dotted areas identify temporal cortex (TCx, upper row), thalamus (TL, middle row) and inferior colliculus (IC, bottom row) at the corresponding level. MicroPET and MRI images were acquired separately at baseline quiet state and fused together. Rat was imaged in prone position. Ant, anterior; Post, posterior; R, Right; L, left.

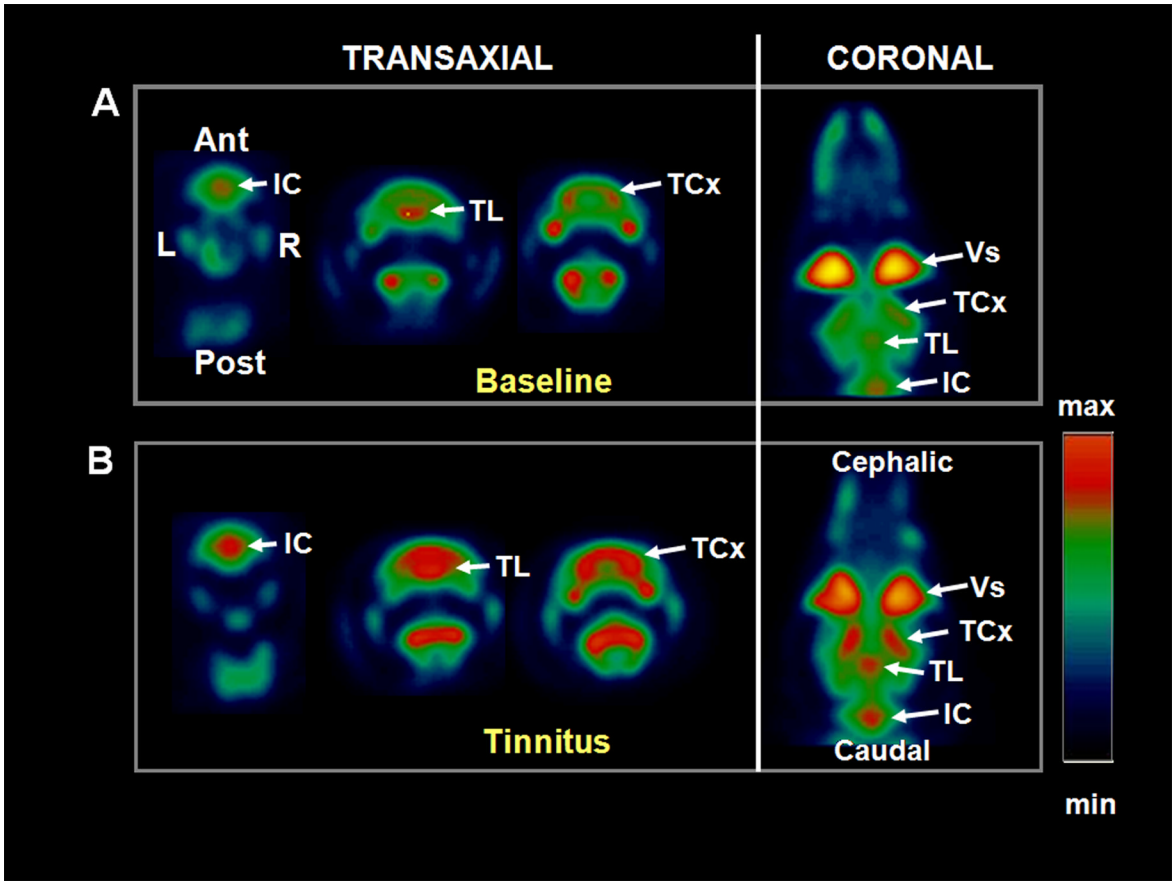

Fig. 5.

MicroPET images of a rat brain showing increase in FDG activity in the inferior colliculi (IC), thalami (TL), temporal cortices (TCx) and periorbital capillaries (Vs) during salicylate-induced tinnitus (B) compared to that at baseline (A). Images are displayed in the identical color scale (right). First 3 columns represent transverse slices and the 4th column represents the coronal slices. Rat was imaged in prone position. Ant, anterior; Post, posterior; R, Right; L, left.

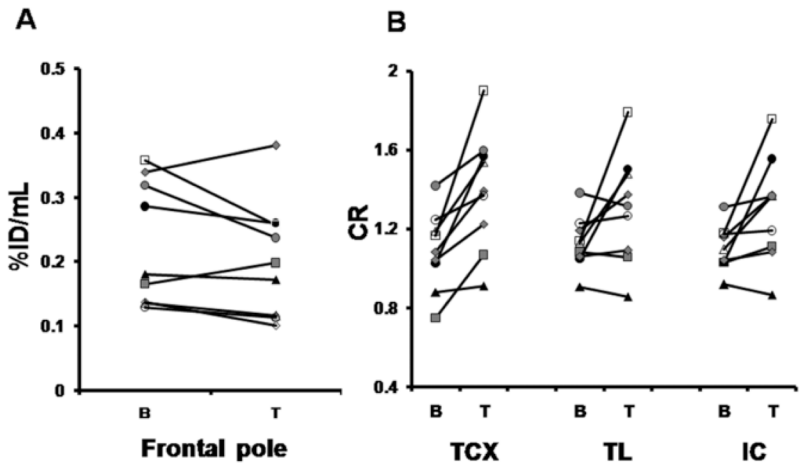

Fig. 6.

Changes in FDG activity from baseline (BL) to tinnitus (T) conditions in the frontal pole (A) and central auditory structures (B) of each of the 9 rats in group 3. FDG activity is expressed as % injected dose per mL (%ID/mL) in the frontal pole and CR (count ratio) in the central auditory structures. Central auditory structures include temporal cortices (TCx), thalami (TL) and inferior colliculi (IC).

Table 1

FDG activity during tinnitus compared to baseline

FDG CR	Temporal cortex	Thalami	Inferior colliculi
Number of rats showing increase	9/9	6/9	8/9
Mean			
Baseline	1.08 ± 0.19	1.13 ± 0.13	1.10 ± 0.12
Tinnitus	1.39 ± 0.29	1.30 ± 0.28	1.30 ± 0.27
p value	0.003	0.07	0.03
Percent change from baseline			
Mean	29 ± 20	16± 23	17 ± 21
Range	4 to + 63	−6 to +57	−6 to 51%

FDG CR= FDG count ratio calculated as FDG count of a structure divided by the FDG count of the frontal pole